JOURNAL OF CATALYSIS 157, 523–535 (1995)

Adsorption, Activation, and Oxidation of Ammonia over SCR Catalysts

Gianguido Ramis,* Li Yi,* Guido Busca,*,[1] Maria Turco,† Elke Kotur,‡ and Ronald J. Willey‡

*Istituto di Chimica, Facoltà di Ingegneria, Università di Genova, P.le J.F. Kennedy, I-16129 Genoa, Italy; †Dipartimento di Ingegneria Chimica, Università "Federico II", P.le Tecchio 80, I-80125 Naples, Italy; and ‡Department of Chemical Engineering, Northeastern University, Boston, Massachusetts 02115

Received December 16, 1994; revised March 21, 1995; accepted June 20, 1995

The catalytic activity in the reduction of NO by ammonia in the presence of oxygen (SCR process) is reported for $CuO–TiO_2$ and for different catalysts belonging to the $MgO–Fe_2O_3$ system. These materials show high activity even at relatively low temperatures, with a maximum NO conversion near 520 K ($CuO–TiO_2$) and 600 K ($MgO–Fe_2O_3$). At higher temperatures, NO conversion is reduced because of the competitive NH_3 oxidation by O_2 to NO_x and N_2. The adsorption and transformation of ammonia over these systems has been investigated by FT-IR spectroscopy in vacuum and in contact with oxygen and NO. In all cases ammonia is first coordinated over Lewis sites and later undergoes hydrogen abstraction giving rise either to NH_2 amide species or to its dimeric form N_2H_4, hydrazine, detected over $CuO–TiO_2$ and γ-Fe_2O_3. Other species tentatively identified as imide NH, nitroxyl HNO, nitrogen anions N_2^-, and azide anions N_3^- are produced further. In the presence of NO, coordinated ammonia rapidly disappears, the above intermediates are not found, and water is produced, showing that the SCR reaction occurred. Ammonia protonation to ammonium ion is not detected at all over these systems. It seems consequently demonstrated that Brønsted acidity is not necessary for the appearance of SCR activity. A comparison with the previously-published data on $V_2O_5–TiO_2$-based systems is done and mechanisms of ammonia oxidation by oxygen and by NO are proposed.

INTRODUCTION

The so-called SCR process is based on the selective catalytic reduction of NO by ammonia, through the main reaction

$$4\ NO + 4\ NH_3 + O_2 = 4\ N_2 + 6\ H_2O. \qquad [1]$$

This process is now well established and is widely used for the abatement of nitrogen oxides from waste gases of stationary sources (1, 2). The industrial catalysts are based on $V_2O_5–TiO_2$ anatase with addition of either WO_3 or MoO_3 (1, 2). These formulations are optimal in order to have sufficient catalytic activity in the SCR reaction, but with limited activity in several concurrent unwanted reactions, like the reduction of NO to N_2O, the oxidation of ammonia to N_2 and NO_x, and the oxidation of SO_2 (frequently present in waste gases) to SO_3 (3). Other catalyst formulations, such as copper-oxide- (4), iron-oxide- (5), chromium-oxide- (6) and manganese-oxide- (7) based catalysts, have been tested (1) and show high or very high catalytic activity for the SCR reaction, but with lower selectivity to N_2, smaller working window, higher conversion of SO_2 to SO_3, and/or lower stability in SO_x-containing environments (8).

The mechanism of the SCR reaction has been investigated over vanadia-based catalysts by several authors. Most of them agree that reaction [1] occurs by activation of ammonia by strong adsorption over the catalyst, while NO reacts from the gas phase or from a weakly adsorbed state (1, 9). However, authors disagree on the activation mode of ammonia over the catalyst. Early studies by Takagi *et al.* (10) and by Miyamoto *et al.* (11) suggested that the active ammonia species over vanadia-based catalysts is in the form of ammonium ions, so activation of ammonia would occur on the surface Brønsted acid sites. The role of ammonium ions as active ammonia species has been supported by more recent investigations (12–14). Alternatively, Janssen *et al.*, on the basis of isotopic labeling experiments, proposed ammonia activation over vanadyl sites giving rise to $V–O–NH_2$ species (15), i.e., formally an adsorbed form of hydroxylamine. This hypothesis has been recently assumed also by Ozkan *et al.* (16). Based on IR experiments over bulk V_2O_5 (17), $V_2O_5–TiO_2$ (18), and $V_2O_5–WO_3–TiO_2$ catalysts (19), a mechanism involving ammonia activation over vanadyl centers giving rise to $-NH_2$ amide species has been suggested. This mechanism, similar to that proposed previously on the basis of a kinetic study over ferric oxide catalysts (20), involves hydrogen abstraction from coordinated ammonia. Other authors

[1] To whom correspondence should be addressed.

0021-9517/95 $12.00

TABLE 1

Surface Areas and XRD Phases of the Catalysts under Study

Notation	Surface area[a]	XRD phase
10% $CuO-TiO_2$	85	anatase (traces of brookite)
α-Fe_2O_3	20	hematite
γ-Fe_2O_3	22	maghemite (defective spinel)
$Mg_{0.4}Fe_2O_{3.4}$	100	defective spinel
$Mg_{0.66}Fe_2O_{3.66}$	129	defective spinel
$MgFe_2O_4$	128	magnesioferrite (inverted spinel)
$Mg_2Fe_2O_5$	83	nonstoichiometric spinel
$Mg_4Fe_2O_7$	80	spinel + MgO
$Mg_6Fe_2O_9$	79	spinel + MgO
MgO	17	periclase

[a] m^2/g.

seem to agree with this conclusion (21, 22) and used this mechanism for kinetic modeling (23).

To obtain further evidence for the mechanism of the SCR reaction [1] we investigated it over active systems other than those based on $V_2O_5-TiO_2$, although their application in the industrial case is ruled out in relation either to their too low selectivity to nitrogen or to their behavior in the presence of SO_2.

In this paper, we report data on ammonia adsorption and activation and on the SCR reaction over catalysts belonging to the $CuO-TiO_2$ and $MgO-Fe_2O_3$ systems.

EXPERIMENTAL

Some data on the catalysts are summarized in Table 1. The $CuO-TiO_2$ catalyst (10% CuO w/w, 85 m^2/g) was prepared by impregnation of Tioxide TiO_2 (anatase with traces of brookite) with copper nitrate, as reported previously (24). The preparation and characterization of Mg-ferrite aerogels has also been described previously (25). The sample γ-Fe_2O_3 is a commercial one from Bayer.

Catalytic experiments with $CuO-TiO_2$ were carried out in a continuous, fixed bed reactor operating at atmospheric pressure (26). The reacting mixture (80 liter/h) contained 650 ppm NO, 650 ppm NH_3, 3% v/v O_2, and Ar as balance. The reactor was loaded with 100 mg of catalysts with grain dimensions of 150–212 μm. NO concentration was measured with a Beckman 955 chemiluminescence NO analyzer. Ammonia concentration was measured with a Uras 3G Hartmann & Braun IR spectrophotometer, while N_2O and N_2 were measured by GP (HP5890 with a double packed Porapak Q molecular sieve column, TCD).

The catalytic experiments over Mg-ferrites were performed in a continuous flow unit, with a 26 mm ID Pyrex glass reactor and 100 mg of catalyst. The inlet gas composition (200 liter/h) was 2000 ppm of NO and 3000 ppm of NH_3 in air. NO conversion was measured with a Thermo Electron Series 44 chemiluminescent NO analyzer. The aerogels were pretreated in situ with flowing air at 773 K for 2 h. N_2O analysis was performed by gas chromatography.

FT-IR spectra were performed with Nicolet 5ZDX and Magna 750 Fourier Transform spectrometers (4 cm^{-1} resolution) using self-supporting pressed disks of the pure catalyst powders, previously pretreated by calcination in the IR cell at 673 K for 2 h and outgassing at 673 K for 30 min. Adsorbates were taken from commercial cylinders from SIAD (Milano, Italy).

RESULTS

(*a*) *Catalytic Activity*

The catalytic behavior of the $CuO-TiO_2$ catalyst is shown in Fig. 1. The catalyst is very active already at 473 K, while its activity increases with a maximum at 523 K. At higher temperatures the activity decreases because of the concurrent fast ammonia oxidation by oxygen, as shown by the increased converted NH_3/converted NO ratio and the presence of N_2O in the reaction products. The selectivity to N_2 is quite high, although the selectivity to N_2O increases with reaction temperature up to near 10%. A comparison with the behavior of vanadia–titania catalysts with vanadia loadings approaching the monolayer in the same conditions (26) shows that the catalytic activity of $CuO-TiO_2$ is comparable or even higher at low temperature, but selectivity to N_2 is lower. The general trend is similar to that reported previously over similar $CuO-TiO_2$ catalysts (4, 27) and agrees with the high catalytic activity of similar catalysts for the oxidation of ammonia by O_2 (28).

In Table 2 the specific rate constant of the SCR reaction per m^2 of catalyst for samples belonging to the $MgO-Fe_2O_3$ system is given. In most cases the NO conversion activity shows a maximum in the range near 600 K and later decreases, going down to negative values, showing that NO is formed by ammonia oxidation by oxygen. In one case, however, two maxima are found. This can be due to the presence of two different sites, one of which is more active than the other in ammonia oxidation by both NO and O_2. The most active catalysts in this series are those constituted by Mg-defect nonstoichiometric spinels. The sample $Mg_{0.4}Fe_2O_{3.4}$ under our conditions gives rise to conversions not far from 80% in the temperature range 550–700 K. Interestingly, the maghemite ferric oxide polymorph (γ-Fe_2O_3) is apparently less active in both SCR and ammonia oxidation by O_2 than the hematite polymorph (α-Fe_2O_3) at the same temperature, but the balance of the activity in the two reactions results in better NO conversions in the range 600–650 K. In all cases no N_2O was detected, within the sensitivity of our equipment.

These data agree with literature data showing that oxide materials containing ferric ions, like Fe_2O_3/Al_2O_3 (5),

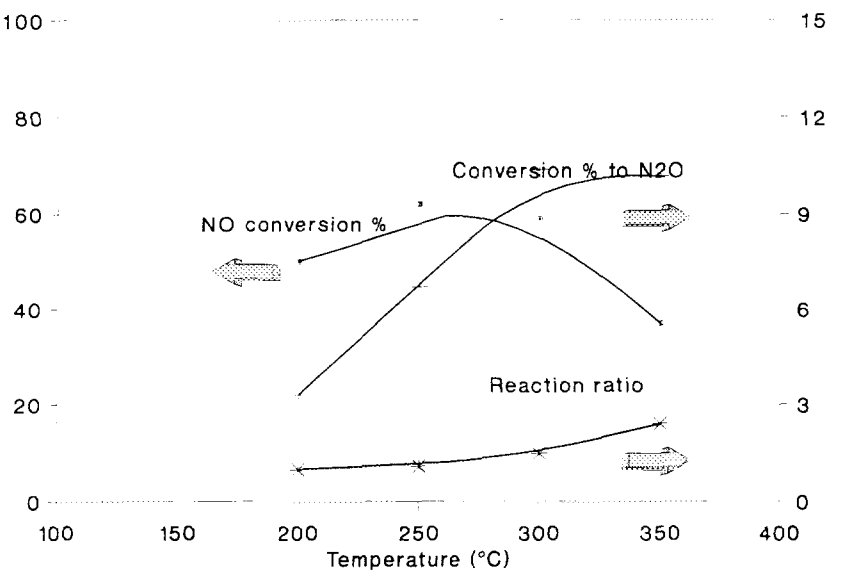

FIG. 1. Catalytic activity of $CuO-TiO_2$.

Fe_2O_3/TiO_2 (29), $Fe_2O_3-SiO_2$ (30), $Fe_2O_3-Cr_2O_3-Al_2O_3$ mixed oxides (31, 32), and Fe-zeolites (33), are active SCR catalysts in the range 500–600 K. For example, Janssen and van den Kerkhof reported on the activity of $Fe_2O_3-SiO_2$ in the SCR reaction, with a maximum NO conversion just near 600 K (30) and a small production of N_2O above this temperature. On the other hand, catalytic systems containing ferric ions have also been found to be active in ammonia oxidation by O_2 giving rise to mainly N_2 at low temperatures (34) and NO at high temperatures (35).

The behavior of both $CuO-TiO_2$ and $MgO-Fe_2O_3$ catalysts seems to be parallel to that of catalysts based on $V_2O_5-TiO_2$, that also show at low temperatures a substantially selective behavior with increasing activity by increasing temperature, and with a maximum followed by a decrease of conversion associated to ammonia oxidation by oxygen. At the temperature at which NO conversion begins to decrease, selectivity to N_2 begins to decrease from 100%, due to N_2O production (36–39).

TABLE 2

First Order Rate Constants k ($m^3/h \cdot m^2$) per m^2 of Catalyst Surface Area for the Selective Catalytic Reduction of NO by Ammonia over Catalysts of the MgO–Fe_2O System

Catalyst	Temperature (K)					
	450	500	550	600	650	700
α-Fe_2O_3	1,230	4,160	5,850	3,720	−10,180	−42,430
γ-Fe_2O_3	0	850	7,590	16,040	20,740	16,670
$Mg_{0.4}Fe_2O_{3.4}$	15	1,782	9,816	28,545	21,044	27,128
$Mg_{0.66}Fe_2O_{3.66}$	239	839	3,920	11,000	6,742	6,004
$MgFe_2O_4$	0	53	1,809	6,782	3,056	2
$Mg_2Fe_2O_5$	616	3,097	8,123	14,265	9,072	−4,302
$Mg_4Fe_2O_7$	152	341	660	746	−464	0
$Mg_6Fe_2O_9$	0	0	644	1,076	−496	−3,101
MgO	0	0	2,100	4,229	1,429	−13,782

Note. Negative rate constants mean that NO is produced by NH_3 oxidation by O_2.

(b) FT-IR Study of Ammonia Adsorption and Activation over $CuO-TiO_2$

The FT-IR spectra of the adsorbed species arising from contact of the $CuO-TiO_2$ catalyst surface with ammonia are reported in Fig. 2. The spectrum after contact at r.t. (Fig. 2a) is dominated by a rather sharp although very strong band at 1602 cm^{-1} and by a slightly weaker one centered at 1160 cm^{-1}, having an additional pronounced component at 1225 cm^{-1}. These two features are associated to the asymmetric and symmetric deformation of ammonia coordinated over Lewis acid sites (40). Correspondingly, bands are found at 3395, 3340, 3250, 3200, and 3140 cm^{-1} in the NH stretching region (as shown in Fig. 4a). The splitting of the symmetric deformation band and of some NH stretchings is associated to the presence of species adsorbed on more than one site. The position of the most sensitive mode, the symmetric deformation, only slightly differs from that measured on the bare support (1215, 1170 cm^{-1} (41, 42)). The evolution with increasing temperature, we will describe below, strongly differs from that observed over the pure TiO_2 support (where only progressive desorption is observed (41, 42)). This indicates that adsorption occurs over the supported CuO_x species typical of the "monolayer" (24).

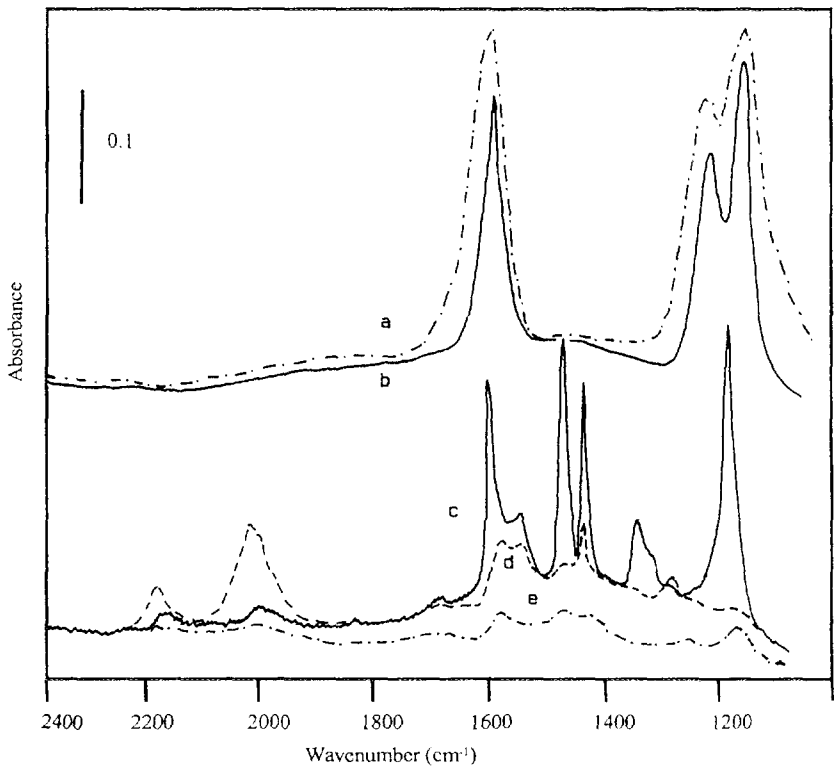

FIG. 2. FT-IR spectra of the adsorbed species arising from NH_3 adsorption (20 Torr) over $CuO-TiO_2$ at (a) r.t. and successive outgassing at (b) 300 K, (c) 423 K, (d) 523 K, and (e) 623 K.

Under these conditions we did not find any band in the regions 3000–2500 cm^{-1} and 1800–1650 cm^{-1}, and we did not detect the strong and broad band near 1450 cm^{-1}, typically found after ammonia absorption over Brønsted acidic solids, where ammonium ions are formed by ammonia protonation. This indicates that the $CuO-TiO_2$ catalyst is not Brønsted acidic, as expected on the basis of the lack of Brønsted acidity both on the pure TiO_2 support (41, 42) and on the pure copper oxide CuO (43).

By outgassing at 423 K (Fig. 2c) the bands due to coordinated ammonia decrease in intensity, as expected. However, surprisingly, in the asymmetric deformation region now only a single sharp band is observed at 1187 cm^{-1}, while also the band near 1600 cm^{-1} is strongly sharpened and shifted to 1611 cm^{-1}. Simultaneously, other sharp bands grow at 1480 and 1440 cm^{-1}, both strong, and at 1346 cm^{-1}, weak. Sharp components are also observed at 1560 and 1325 cm^{-1}. These spectra strongly suggest that coordinated ammonia transforms by heating into more than one species. This reactivity is not observed at all over the bare support, and consequently involves reaction of ammonia related to the surface CuO phase.

The bands at 1440 and 1480 cm^{-1} apparently correspond to two different species, one of which (1440 cm^{-1}) is formed first and disappears later. The band at 1480 cm^{-1} instead forms and disappears quickly, so it is possibly associated to a species intermediate with respect to the formation of other species. The assignment of these bands will be attempted below.

Finally, the bands found at 1612, 1560, 1345, 1325, and 1187 cm^{-1}, apparently behaving in parallel with each other should correspond to a species formed by "aggregation" of more than one ammonia fragment. These bands closely correspond to those observed on hydrazine complexes like $FeCl_2 \times 2\ N_2H_4$ (44), $ZnCl_2 \times 2\ N_2H_4$ (45), and for hydrazine adsorbed on a Fe/MgO catalyst (46) as shown in Table 3. To have a confirmation of this hypothetical assignment we investigated also the adsorption of hydrazine over our catalyst. The spectra recorded after contact of the activated surface with hydrazine vapor at r.t. and outgassing at increasing temperatures (Fig. 3) show a surprising similarity with those obtained after ammonia adsorption and oxidation. The spectra observed from hydrazine show the bands at the same positions as those from ammonia (within shifts ≤ 3 cm^{-1}) and very similar relative intensities. This supports the above identification of hydrazine as an ammonia oxidation product and also shows that the other species formed by ammonia transformation are also given by hy-

TABLE 3

IR Spectra of Hydrazine Species

$CuO-TiO_2$ adsorbed	γ-Fe_2O_3 adsorbed	Fe/MgO adsorbed Ref. (46)	$FeCl_2 \times 2$ N_2H_4 Ref. (44)	$ZnCl_2 \times 2$ N_2H_4 Ref. (45)	N_2H_4 liq. Ref. (47)	Assign. Ref. (45)
1611	1612	1605	1607	1610	1608	NH_2 scissoring
1560	(1580)	1500	1575	1570	1608	NH_2 scissoring
1346	1360		1351	1345	1324	NH_2 wagging
1325			1307	1310	1283	NH_2 wagging
1187	1221	1205	1179	1170	1098	N–N stretching
	1185	1165	1164	1150	1042	NH_2 rocking
			1156			

drazine transformation. Hydrazine is also responsible for a sharp band at 3080 cm^{-1} (NH stretching), found after ammonia adsorption and transformation.

At 523 K, both after ammonia and hydrazine transformation, all the above bands have strongly decreased or disappeared, but new bands are found near 2200 and 2030 cm^{-1}. These bands are due to species formed by further transformation of the above species. They should necessarily be due either to the stretching mode of a diatomic molecule with nearly a triple bond or, alternatively, to the asymmetric stretching of a linear triatomic molecule. An assignment to triatomic species implies the detection of another band due to the corresponding symmetric stretching mode. From Fig. 2d it seems evident that a third band at lower frequency, namely near 1280 cm^{-1}, also grows simultaneously with these higher frequency bands. So, a very reasonable assignment for the bands at 2030 and 1280 cm^{-1} is to a nearly free azide N_3^- species, by analogy with the bands of KN_3 (2041 and 1344 cm^{-1} (48)). As for the band near 2200 cm^{-1}, a possible assignment to NO^+ species is ruled out by experiments of NO adsorption (see below). The band near 2200 cm^{-1} is formed by ammonia transformation slightly before those assigned previously to azide species. The most reasonable assignment is to dinitrogen anion

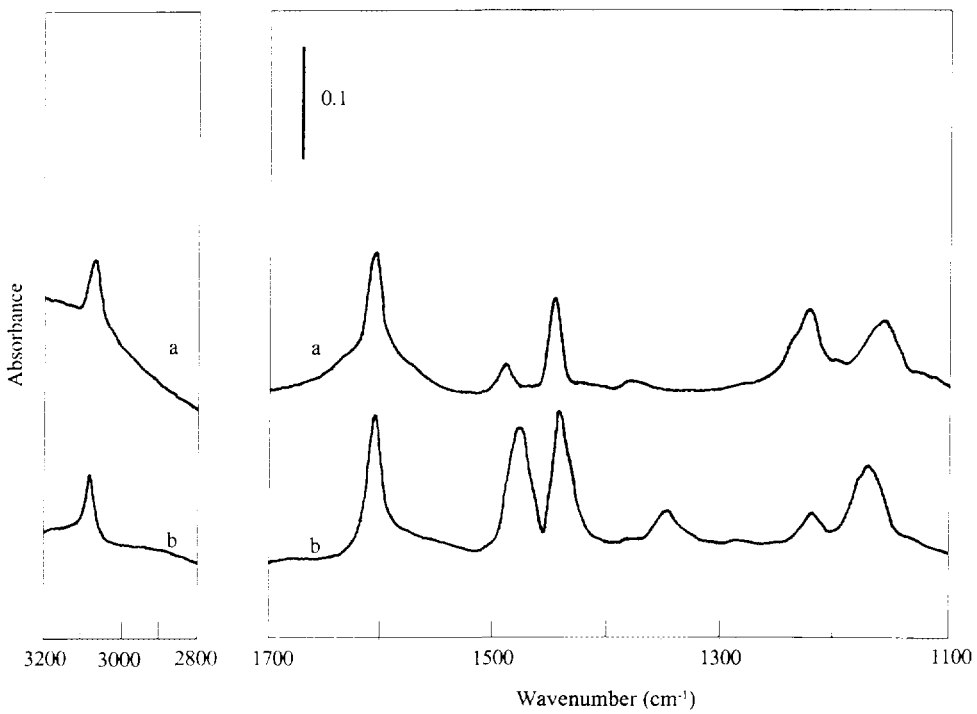

FIG. 3. FT-IR spectra of the adsorbed species arising from the contact of hydrazine vapor with $CuO-TiO_2$ and further outgassing at (a) r.t. and at (b) 423 K.

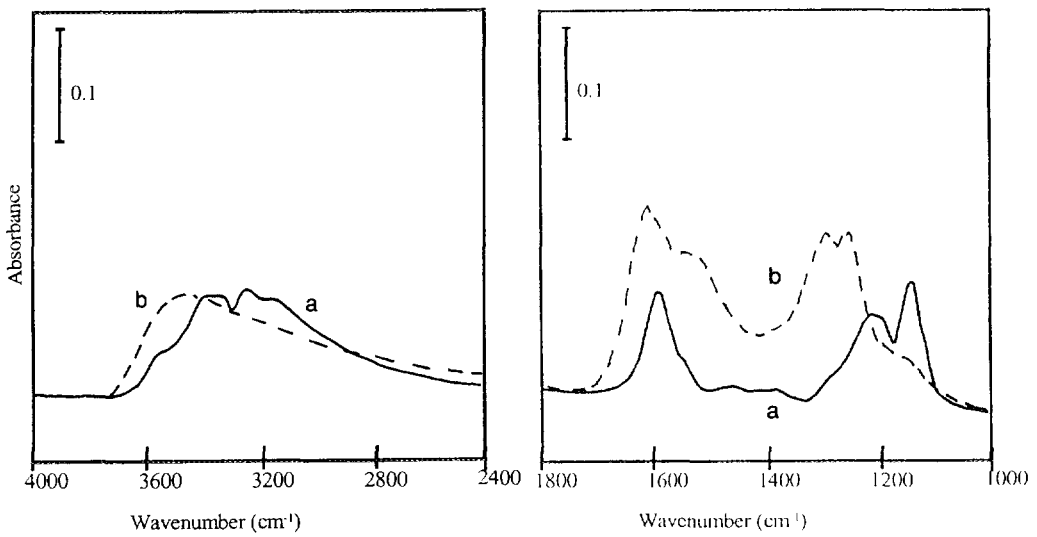

FIG. 4. FT-IR spectra of the adsorbed species arising from NH_3 adsorption (20 Torr) over $CuO-TiO_2$ at r.t. and successive outgassing at (a) 300 K, and from further interaction with NO 20 Torr at (b) 423 K.

N_2^- complexes, in agreement with the recent data of Martra *et al.* (49).

These assignments find additional support on the experimental evidence that the bands above 2000 cm^{-1} are not found if ammonia is heated in contact with NO gas instead of in vacuum (Fig. 4). In fact, NO reacts with adsorbed ammonia at lower temperatures and gives nitrogen and water, through the so called SCR reaction (see below).

(c) *NO Adsorption and NO/NH_3 Coadsorption over $CuO-TiO_2$*

The interaction of NO with activated $CuO-TiO_2$ (Fig. 5) gives rise to a strong band at 1895 cm^{-1}, with a weaker one at 2135 cm^{-1}. Outgassing causes the fast decrease of the intensity of the band at 1895 cm^{-1}, while the other resists short outgassing at r.t. but disappears at higher temperatures. The main band at 1895 cm^{-1} is found at slightly higher frequency with respect to the NO stretching of gaseous NO (1880 cm^{-1} (50)) and can be assigned to surface metal-nitrosyl species. This band resembles, for its position, the main one observed over the bare support (1900 cm^{-1} (42)), although over the bare support another component near 1915 cm^{-1} is also found. Previous data on CO adsorption over the same catalyst (24) indicated that nearly free Ti^{4+} cations are indeed exposed over this surface. However, it seems not excluded that NO over copper cations can give nitrosyls with nearly the same stretching frequency. According to Spoto *et al.* (51), Cu^{2+}–NO species over ZSM5 zeolite are characterized by a single band just at 1895 cm^{-1}. The other band is instead definitely not observed over the pure support. The band at 2135 cm^{-1}, associated to a species more stable to outgassing than the

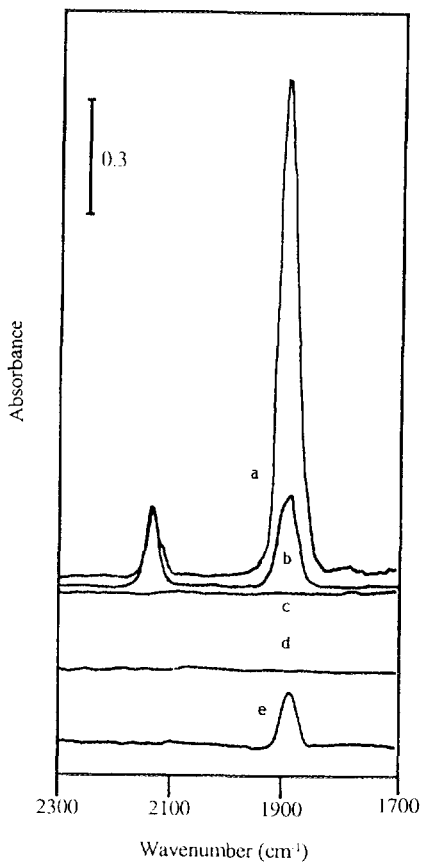

FIG. 5. FT-IR spectra of the adsorbed species arising from NO (20 torr) adsorption over clean $CuO-TiO_2$ at (a) r.t. and successive outgassing at (b) 300 K and (c) 423 K; and from NO interaction with ammonia precovered $CuO-TiO_2$ at (d) r.t. and at (e) 423 K.

previous one, can be assigned to NO^+ species, likely due to the reaction of NO with Cu^{2+} sites, so giving rise to a Cu^+–NO^+ species. This assignment is supported by the similar frequency for the CO stretching of the isoelectronic Cu^+–CO complex observed over the same catalyst (2112 cm^{-1}) and similarly stable to outgassing at r.t. (24).

If NO is put into contact at r.t. with a CuO–TiO_2 surface previously covered by ammonia and outgassed at r.t., the above bands are not observed at all (Fig. 5d), likely due to the "poisoning" of the adsorbing sites by coordinated ammonia. However, after contact with NO already at 423 K the spectra show a strong decrease of the bands due to coordinated ammonia (very evident for the NH stretchings near 3400 cm^{-1} and for the deformations at 1225 and 1160 cm^{-1} (Fig. 4b)) while absorptions grow in the region 3600–3400 cm^{-1} and at 1620 cm^{-1}, typically due to the formation of surface OH's and adsorbed water. Simultaneously bands due to NO oxidation products are also found in the region 1600–1200 cm^{-1}.

Under these conditions, the band at 1895 cm^{-1}, due to surface nitrosyl species, appears again, although weak. These data strongly suggest that NO reacts with coordinated ammonia giving rise to adsorbed water, together with nitrogen, that desorbs and cannot be detected by IR in the gas phase. This frees some of the surface cationic sites where NO can adsorb, giving rise to the band at 1895 cm^{-1} (Fig. 5e). It is remarkable that in the presence of NO the multiple bands observed when ammonia alone interacts and is oxidized are not found at all.

These data strongly support the following points:

(i) Ammonia is adsorbed more strongly than NO over CuO–TiO_2 like over V_2O_5–TiO_2 (18).

(ii) Coordinated ammonia reacts with NO giving rise to water, so the SCR reaction is observed in our cell already starting at 423 K. The occurrence of this reaction agrees with the catalytic measurements reported above.

(iii) The lack of detection, in the presence of NO, of the complex chemistry observed when ammonia is adsorbed alone is due to the fast reaction of ammonia (or of one of its very first transformation products) with NO. This reaction should be faster than the above-described ammonia fragmentation and "aggregation" to produce different oxidation species including hydrazine N_2H_4. So, the first intermediate very reasonably involved in the reaction with NO is the reactive species amide NH_2 that in the absence of NO can dimerize to N_2H_4, while in the presence of NO can give $N_2 + H_2O$.

(*d*) *FT-IR Study of Ammonia Adsorption and Activation over MgO–Fe_2O_3 Catalysts*

The spectrum of ammonia adsorbed at room temperature on the stoichiometric spinel $MgFe_2O_4$ (Fig. 6a) is characterized by bands at 1606 and 1172 cm^{-1} (asymmetric and symmetric deformation of coordinated NH_3), with additional components at 1636 and 1130 cm^{-1} that can be assigned to ammonia H-bonded over basic sites (40). After outgassing at 473 K the molecular adsorbed forms of ammonia are almost gone; while a broad band is clearly formed at 1550 cm^{-1}, another sharper band is formed at 1425 cm^{-1} together with a sharp doublet at 2195, 2175 cm^{-1} (Fig. 6b). If contact is carried out directly at higher temperatures, e.g., 473 K (Fig. 6c), sharp bands predominate at 2195, 2175 (doublet), 1565 (shoulder), and 1425 cm^{-1} (sharp). The spectra on $MgFe_2O_4$ can be discussed taking into account those previously reported for ammonia adsorption and oxidation over α-Fe_2O_3 (52) and MgO (49, 53). According to these previous studies, the relatively broad band near 1560 cm^{-1} is certainly due to the scissoring mode of an amide species M-NH_2, the sharper one at 1425 cm^{-1} is due to the bending of imido M-NH species and the split band near 2180 cm^{-1} is assigned to the N≡N nearly triple bond stretching of N_2^- ions. From the experiments reported in Fig. 6, it seems clear that amide species are formed from coordinated ammonia, and that both N_2^- species and imido-species arise from amide species. The picture is quite similar to that reported previously for adsorption over α-Fe_2O_3 (52), where also amide, imide, and N_2^- species were found after heating of adsorbed ammonia.

Over the Mg-deficient spinel $Mg_{0.66}Fe_2O_{3.66}$ (Fig. 7) ammonia adsorption gives again bands at 1602 and 1190 cm^{-1}, due to coordinated ammonia, without any evidence of ammonium ions. A shoulder at 1635 cm^{-1} is due to ammonia H-bonded over basic sites. However, a couple of bands grow already at r.t. by increasing contact time at 1470 and 1404 cm^{-1}, while a split band also grows at 2193, 2184 cm^{-1}. These bands are even more evident after outgassing at 473 K, although the couple of bands in the region 1500–1400 cm^{-1} completely disappears at higher temperatures.

The analysis of the spectra indicates that the band near 1470 cm^{-1} is formed more slowly than that at 1404 cm^{-1} (likely due to an imido species), but successively it grows faster and disappears also faster. So this species seems to be associated to a real intermediate species between the amide NH_2 and nitrogen or other volatile species like NO.

In any case, the detection of the imido species and of N_2^- species already at r.t. agrees with the higher catalytic activity of this catalyst with respect to $MgFe_2O_4$ (see above).

The spectrum of ammonia adsorbed at r.t. over γ-Fe_2O_3 (Fig. 8) is similar to that observed previously over the α-Fe_2O_3 polymorph. It consists of a pointed but rather broad band at 1603 cm^{-1}, due to the asymmetric NH_3 stretching, and of a stronger and even broader band centered near 1230 cm^{-1}. The spectrum is cut in the region 1400–1300 cm^{-1} because of the presence of a negative band at 1362 cm^{-1} due to the perturbation of the S=O band of traces

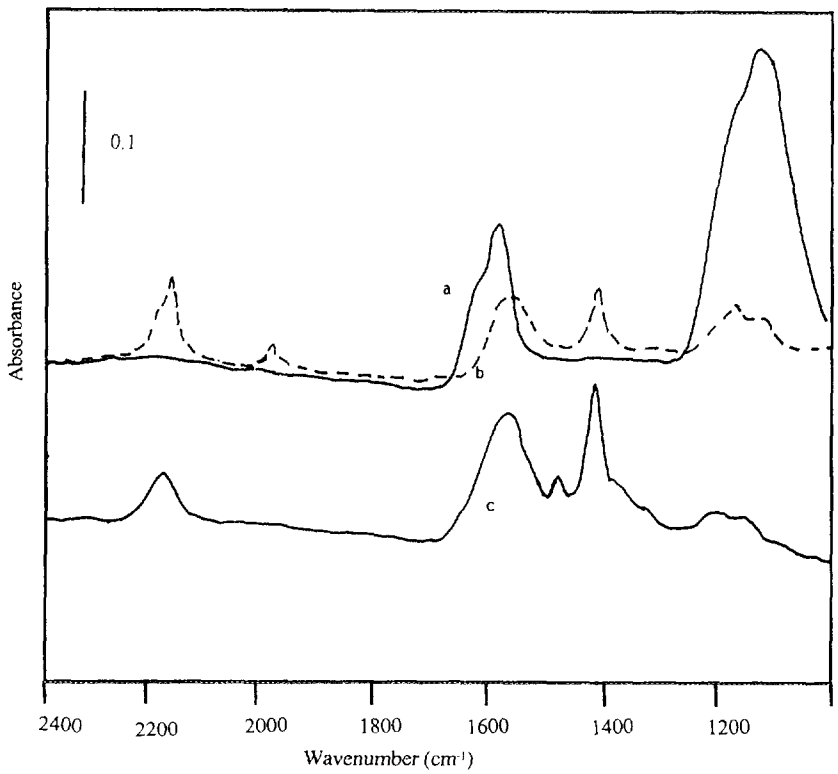

FIG. 6. FT-IR spectra of the adsorbed species arising from NH_3 adsorption (20 Torr) over $MgFe_2O_4$ at (a) r.t. and successive outgassing at (b) 473 K, and from NH_3 interaction (20 Torr) over $MgFe_2O_4$ at (c) 473 K.

of sulphates present as an impurity over this sample. No bands were observed at r.t. in the regions 1700–1650 cm^{-1} and 1500–1400 cm^{-1}, showing that ammonium ions were not formed. This confirms previous data on both ferric oxide polymorphs (52, 54) that showed no Brønsted acidity.

After outgassing at 373 K the spectrum is deeply modified. Only very sharp bands were observed at 1610, 1450, 1220, and 1190 cm^{-1}. These bands persist after outgassing at 473 and 573 K, but the sharp band at 1450 cm^{-1} is substituted by a couple of slightly broader bands at 1473 and 1445 cm^{-1}.

The comparison of the features observed over $MgFe_2O_4$ and $Mg_{0.66}Fe_2O_{3.66}$ with those observed on γ-Fe_2O_3 allows us to assign the band near 1445 cm^{-1} to an imide NH species. So, the same assignment can be given for the species responsible for the band detected at 1440 cm^{-1} over $CuO–TiO_2$ (see above). Instead, the band at 1475 cm^{-1} should correspond to the same intermediate, observed also on the nonstoichiometric Mg-ferrite and over $CuO–TiO_2$. A tentative assignment for this species will be proposed below. However, on γ-Fe_2O_3 another species should be present, responsible for very sharp bands at 1612, 1220, and 1190 cm^{-1}. These features could correspond to coordinated ammonia, surprisingly stable to heating. However, the sharpness of these features is unusual. Moreover, sharp and weak components can be also be found near 1580 and 1360 cm^{-1} (the latter superimposed to the bands of sulphate impurities) and can be due to the same species. These features look like those observed above over the $CuO–TiO_2$ catalyst, certainly due to adsorbed hydrazine species (Table 3). So, they can be assigned to adsorbed hydrazine formed by ammonia oxidative dehydrogenation also on γ-Fe_2O_3. Hydrazine over on γ-Fe_2O_3 disappears after heating at 623 K.

NO adsorption over these systems gives rise to nitrosyl complexes characterized by the NO stretching in the region 1830–1790 cm^{-1}. These complexes are weakly bonded and do not form if ammonia is previously adsorbed. Contact of NO with ammonia-precovered surfaces in the temperature range 300–500 K produces the progressive disappearance of coordinated ammonia and the formation of water, in a similar way as previously described for $CuO–TiO_2$. So, analogous conclusions can be reached.

DISCUSSION

The experiments performed by using $CuO–TiO_2$ and different $MgO–Fe_2O_3$ powders as catalysts for the catalytic reduction of NO by ammonia show that these materials are active in the temperature range 400–700 K. These

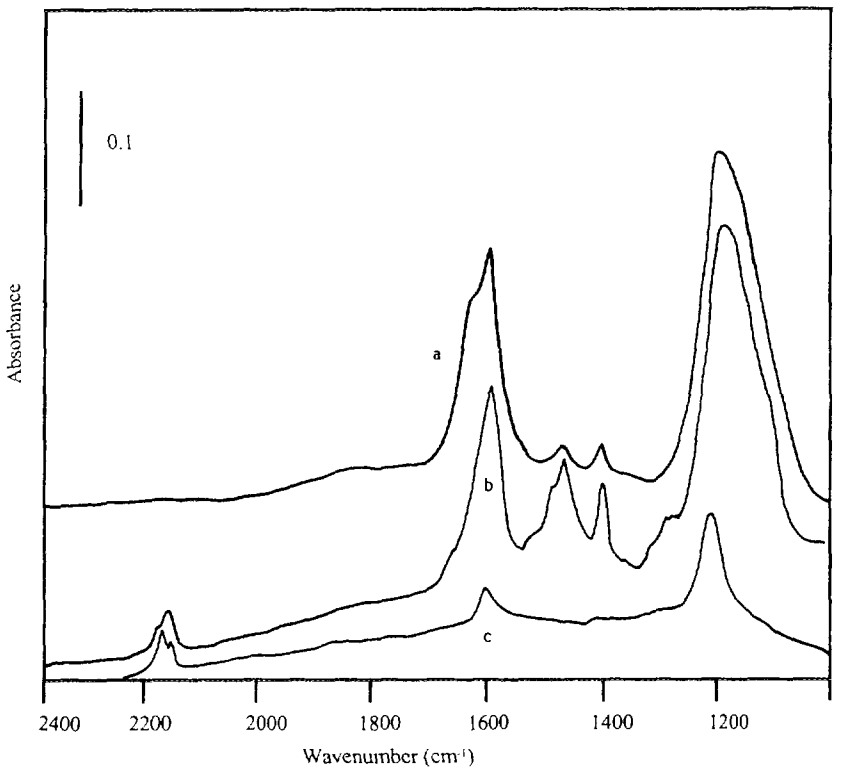

FIG. 7. FT-IR spectra of the adsorbed species arising from NH_3 adsorption (20 Torr) over $Mg_{0.66}Fe_2O_{3.66}$ at (a) r.t. and successive outgassing for 10 min at (b) 300 K and for 10 min at (c) 473 K.

data confirm those already reported in the literature for $CuO-TiO_2$ systems (4, 27) as well as for a number of other Fe_2O_3-based catalysts (5, 29–32). A rough comparison between the catalytic activities of these systems with the $V_2O_5-TiO_2$ based systems indicate that the working window of these catalysts is likely smaller than that of industrial vanadia–titania-based catalysts, mainly because of the higher activity in ammonia oxidation by oxygen found over our systems. However, at relatively low temperatures these systems appear to be active and selective catalysts for the SCR process.

Previous IR studies of ammonia adsorption over vanadia–titania systems (13, 17, 18) showed that ammonia adsorbs in two different forms, i.e., coordinated ammonia on Lewis acid sites and ammonium ions on Brønsted acid sites. From this, the question arises of which is the active site for ammonia activation over these systems. Our spectroscopic results convinced some of us that the active ammonia species over vanadia–titania systems is the coordinated form of ammonia (17–19), with protonated ammonia being essentially a spectator species. However, other authors have the opposite opinion (10–14).

Concerning ammonia adsorption over $CuO-TiO_2$ and $MgO-Fe_2O_3$, IR spectra show clearly that ammonia is not protonated at all. This corresponds to the lack of Brønsted acidity found on the simple oxides CuO (43) and TiO_2 (41, 42), as well as MgO (40, 49, 53) and Fe_2O_3 (52, 54). This contrasts with the Brønsted and Lewis acidity of pure V_2O_5 (55), the active component in the industrial SCR catalysts.

The main conclusion is consequently that ammonium ions do not exist over $CuO-TiO_2$ and $MgO-Fe_2O_3$ and consequently cannot act as the active species in the SCR process over these materials. On the other hand, the above data show without doubt that ammonia, first coordinated over Lewis sites, undergoes deep transformation over all of these systems, in the absence of NO. Although the spectra observed are very complex and only tentative assignments can be given to some of the observed bands, both on spectroscopic and on chemical bases, some other data are unequivocal.

In particular, over all of these surfaces ammonia is rather easily deprotonated giving rise either to a NH_2 amide species, well evident in the absence of NO over α-Fe_2O_3 and $MgO-Fe_2O_3$ mixed oxides, or to its dimeric form N_2H_4, hydrazine, observed over $CuO-TiO_2$ and γ-Fe_2O_3.

Over all catalysts discussed here, two other species are observed to form both in ammonia and hydrazine transformation, one of which is formed rather easily and character-

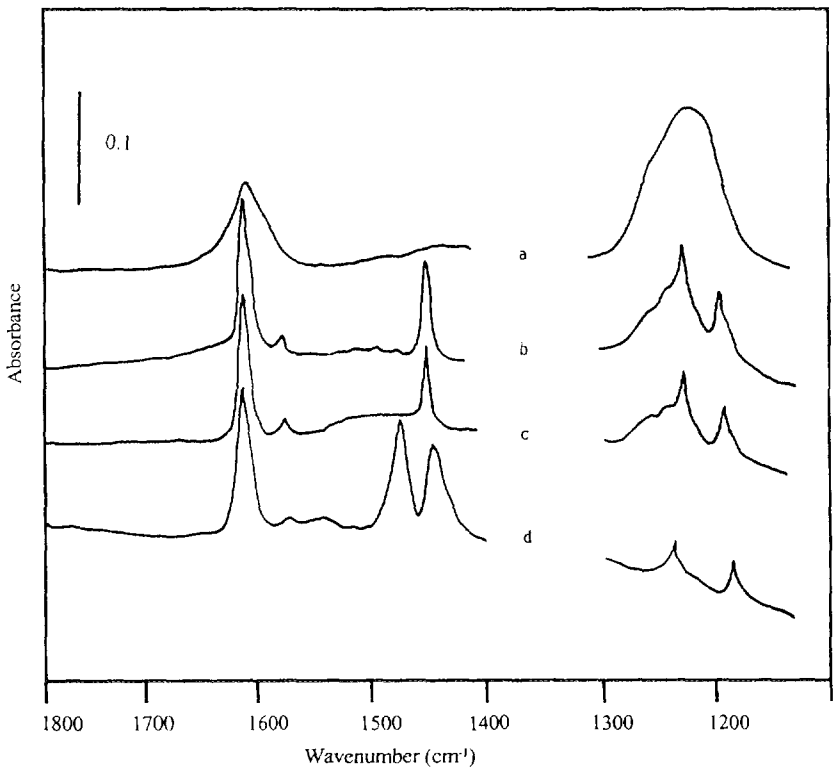

FIG. 8. FT-IR spectra of the adsorbed species arising from NH_3 adsorption (20 Torr) over γ-Fe_2O_3 at r.t. and outgassing at (a) r.t., at (b) 373 K, (c) 473 K, and (d) 573 K.

ized by a band in the region 1450–1400 cm^{-1}. This band can be assigned to the NH deformation of imido-species, likely bridging over two or three cations, in agreement with literature data (40, 49, 53). The other one is formed later and is characterized by a band near 1480 cm^{-1}. This band forms relatively slowly but also disappears fast, so it is likely a very reactive intermediate. The assignment of this species is not easy at the moment. In our previous study of NO and ammonia coadsorption over V_2O_5–TiO_2 we also found the formation of a sharp band at 1490 cm^{-1}, and we tentatively assigned it to the N=O stretching of a nitrosamide species NH_2NO (18). In the present case a similar intermediate could also occur. In any case, according to the IR spectra of inorganic (50) and organic (56) N-containing compounds, this band should be due to a N=N or N=O double bond stretching. On the other hand, the study of NO, NO_2, and N_2O adsorption over these systems seems to rule out a possible assignment to nitrogen oxides as well as to nitrite and nitrate species. We can tentatively propose it to be to the N=O stretching of something like an adsorbed HNO species (nitroxyl), intermediate for the production of NO, the main ammonia oxidation product at high temperature. This molecule is reported to show the NO stretching at 1570 cm^{-1} when isolated in inert gas matrices (50), but upon interaction with the surface this band can be very reasonably shifted down strongly.

Finally, over these catalysts terminal strongly adsorbed transformation products of ammonia are observed and have been identified on the basis of literature data as N_2^- and N_3^- species.

The above data show that the fragments produced by ammonia dissociation tend to "condense." So, N_2, undetectable by IR and easily desorbed, is likely the primary product of the surface reaction we were observing, while N_2^- can be taken as a strongly adsorbed form of it.

So a mechanism like the following (where only adsorbed species are considered, for simplicity) can be proposed for the surface reactions observed by ammonia oxidation in the absence of NO:

$$NH_3 \rightarrow NH_2 + e + H^+ \quad [2]$$

$$2\,NH_2 \rightarrow NH_2\text{–}NH_2 \quad [3]$$

$$NH_2\text{–}NH_2 \rightarrow N_2 + 4\,H^+ + 4\,e \quad [4]$$

$$2\,H^+ + O^{2-} \rightarrow H_2O. \quad [5]$$

Obviously, the electrons produced by these "oxy-dehy-

drogenation" reactions are assumed by reducible cations (Cu^{2+} and Fe^{3+}) that are just reduced. In the presence of oxygen these sites are reoxidized, giving rise to

$$1/2\ O_2 + 2\ e \rightarrow O^{2-}. \qquad [6]$$

The reaction sum $2 \times [2] + [3] + [4] + 3 \times [5] + 3 \times [6]$ gives rise to the overall reaction

$$2\ NH_3 + 3/2\ O_2 \rightarrow N_2 + 3\ H_2O, \qquad [7]$$

i.e., the selective catalytic oxidation of ammonia to N_2 by oxygen (SCO process). Interestingly, $CuO-TiO_2$-based catalysts have been proposed for this reaction (28).

The reaction mechanism [2] to [6] has features in common to that proposed some years ago by Williamson *et al.* to occur over Cu-exchanged zeolites (57), where the slow step in excess of oxygen was found to be reaction [2], i.e., the reduction of Cu(II) to Cu(I) by ammonia. The above mechanism seems also roughly consistent with the data of Bierman and Janssen that investigated the selective oxidation of ammonia by O_2 over MoO_3/SiO_2 catalysts and detected the presence of N- and H-containing adsorbed species as reaction intermediates (58), as well as with some conclusions of de Boer *et al.* (59) over the same system. Finally, this mechanism agrees with that proposed to occur over chromia surfaces (22). On the other hand, this mechanism is also supported by the known chemistry of hydrazine, that can be produced by ammonia oxidation and is further oxidized easily to N_2 by transition metal cations in a high oxidation state like Mo(VI), V(V) and Cr(VI) possibly with the intermediacy of diimide (60). This mechanism is of the so-called Mars–van Krevelen or redox type (61), so implying the reduction of the surface by the reducing agent and its reoxidation by oxygen, with no involvement of adsorbed oxygen species.

The side reactions

$$NH_2 \rightarrow NH + H^+ + e \qquad [8]$$

$$NH + O^{2-} \rightarrow HNO + 2\ e \qquad [9]$$

$$HNO \rightarrow NO + H^+ + e \qquad [10]$$

can give rise to NO, the main product of ammonia oxidation at high temperatures, formed easily in particular over Fe_2O_3-based materials. Also this suggested mechanism is of the Mars–van Krevelen type. However, recently, oxidation of ammonia has been investigated over MgO–CoO solid solutions by Escalona-Platero *et al.* (62) and a reaction of amide species with adsorbed superoxide species producing nitrite and nitrate species was evident. These anions are likely precursors for NO. This result agrees with the high activity in ammonia oxidation to NO of MgO-rich samples belonging to the $MgO-Fe_2O_3$ system including pure MgO (Table 3), for which a Langmuir–Hinshelwood mechanism is likely. In effect, the involvement of molecular oxygen in ammonia oxidation to NO over oxides has been proposed by other authors (34) and cannot be excluded to be active also over our systems.

These mechanisms should occur in the absence of NO. In the presence of NO we cannot detect these species (in particular hydrazine, imide, and nitroxyl) but we observe a rapid decrease of the bands due to coordinated ammonia and the formation of adsorbed water. This behavior can be interpreted assuming that a new fast reaction occurs in the presence of NO:

$$NH_2 + NO \rightarrow N_2 + H_2O. \qquad [11]$$

This is what we previously proposed as a key step in the SCR process over vanadia–titania and similar catalysts (17–19). A side reaction like

$$NH + NO \rightarrow N_2O + H^+ + e \qquad [12]$$

can be responsible for N_2O production by reaction of NO with ammonia, according to Duffy *et al.* (22). However, it must be mentioned that N_2O can also be produced from NO in the absence of ammonia and from ammonia alone both in the presence and in the absence of NO.

Reaction [11] is likely faster than reaction [3] if NO is present, at least at low temperatures. This reaction, that likely has an intermediate step in the production of a nitrosamide-like intermediate, frees the cation, now reduced, to be reoxidized by oxygen (reaction [6]). This makes the SCR reaction faster than the SCO of ammonia, so allowing it to occur. This is also supported by the work of Bierman and Janssen (58) that showed that the same N- and H-containing surface intermediates over MoO_3/SiO_2 could react either with oxygen or with NO giving rise mainly to N_2 and H_2O in both cases. Interestingly, with this scheme in mind, we can propose that the first hydrogen abstraction from ammonia is both in the case of SCR and in the case of SCO a slow step. In the latter case it should represent the rate determining step (according to Williamson *et al.* over Cu-zeolite (57)). In the case of the SCR process most authors agree that the reaction order is nearly 0.8 with respect to NO at low temperature (23, 63) and in excess of ammonia, while first order with respect to NH_3 in excess of NO. This could be interpreted by assuming that the first step influences the reaction rate also in the excess of ammonia, thus being a slow step (64).

The data reported here allow us to propose the reaction

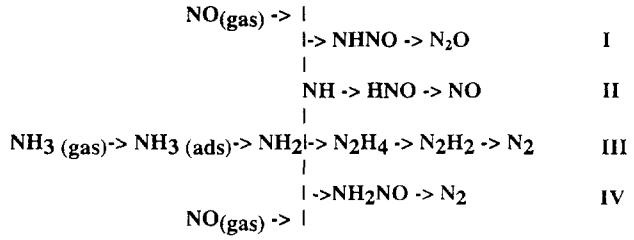

Scheme 1. Proposed reaction scheme for NH_3 oxidations by O_2 (paths II and III) and by NO (paths I and IV).

Scheme 1 concerning Cu- and Fe-containing catalysts, where the SCR reaction is competitive with ammonia oxidation by NO through the common intermediate amide NH_2. Their extrapolation to other systems, like vanadia-based systems is certainly not straightforward. However, to our knowledge data are not available that support the statement that the SCR mechanism is different in these cases. In contrast, a strong parallelism can be found between the catalytic behavior of these systems.

CONCLUSIONS

The main results of this investigation can be summarized as follows:

(i) $CuO–TiO_2$, γ-Fe_2O_3, $Mg_{0.66}Fe_2O_{3.66}$, and $MgFe_2O_4$ catalysts are all active in the catalytic reduction of NH_3 by ammonia at rather low temperatures, although their working windows are likely smaller than in the case of vanadia–titania-based catalysts because of their high activity in ammonia oxidation by oxygen.

(ii) These materials do not show any Brønsted acidity, ammonium ions not being formed by ammonia adsorption.

(iii) In all of these cases ammonia coordinates molecularly over Lewis acid sites but also easily transforms by hydrogen abstraction giving rise either to amide NH_2 species or to its dimeric form hydrazine N_2H_4. Both these species are likely intermediates in the production of N_2 through ammonia oxydation by O_2 (SCO reaction).

(iv) Other ammonia transformation products are clearly found and are identified (with a higher or lower certainty degree) as imide NH species, nitroxyl HNO, nitrogen anions N_2^-, and azide ions N_3^-.

(v) A reaction path from NH_3 to NO via amide–imide–nitroxyl is proposed.

(vi) Gas-phase NO reacts with coordinated ammonia, causing its fast disappearance. During this process water appears.

(vii) These data strongly support a mechanism of the reaction between NO and ammonia (SCR reaction) occurring via coupling of gas-phase or weakly adsorbed NO with an amide species, like previously proposed to occur over vanadia–titania.

(viii) In any case, it is demonstrated that Brønsted acidity is not necessary for low-temperature SCR activity.

ACKNOWLEDGMENTS

This work has been supported in part by NATO (C.R.G. No. 900463) and by MURST (Rome, Italy). Li Yi acknowledges the Chinese and Italian governments for a grant.

REFERENCES

1. Bosch, H., and Janssen, F., *Catal. Today* **2,** 369 (1988).
2. "Proceedings of EPA-EPRI Joint Symposium on Stationary Combustion NO_x Control, Washington, 1991," EPA, Washington, DC, 1991.
3. Svachula, J., Alemany, L. J., Ferlazzo, N., Forzatti, P., Tronconi, E., and Bregani, F., *Ind. Eng. Chem. Res.* **32,** 826 (1993).
4. Iizuka, T., Ikeda, H., and Okazaki, S., *J. Chem. Soc. Faraday Trans. I* **82,** 61 (1986).
5. Wu, S. C., and Nobe, K., *Ind. Eng. Chem. Prod. Res. Dev.* **16,** 136 (1977).
6. Niiyama, H., Murata, K., Ebitani, A., and Echigoya, E., *J. Catal.* **48,** 194 and 201 (1977); Curry-Hyde, H. E., Musch, H., Baiker, A., Schraml-Marth, M., and Wokaun, A., *J. Catal.* **113,** 397 (1992).
7. Kapteijn, F., Singoredjo, L., Dekker, N. J. J., and Moulijn, J. A., *Ind. Eng. Chem. Res.* **32,** 445 (1993).
8. Kittrell, J. R., Eldridge, J. W., and Conner, W. C., *in* "Catalysis," Vol. 9, p. 126. The Royal Society of Chemistry, London, 1992.
9. Srnak, T. Z., Dumesic, J. A., Clausen, B. S., Tornquist, E., and Tøpsøe, N. Y., *J. Catal.* **135,** 246 (1991).
10. Takagi, M., Kowai, T., Soma, M., Onishi, T., and Tamaru, K., *J. Catal.* **50,** 441 (1977).
11. Miyamoto, A., Kobayashi, K., Inomata, M., and Murakami, Y., *J. Phys. Chem.* **86,** 2945 (1982).
12. Chen, J. P., and Yang, R. T., *Appl. Catal. A: General* **80,** 135 (1992); *J. Catal.* **139,** 277 (1993).
13. Topsoe, N. Y., *J. Catal.* **128,** 499 (1991); Topsoe, N. Y., Topsoe, H., and Dumesic, J. H., *J. Catal.* **151,** 226 and 241 (1995).
14. Schneider, H., Tschudin, S., Schneider, M., Wokaun, A., and Baiker, A., *J. Catal.* **147,** 5 (1994).
15. Janssen, F., van den Kerkhof, F., Bosch, H., and Ross, J., *J. Phys. Chem.* **91,** 5931 and 6633 (1987).
16. Ozkan, U. S., Cai, Y., and Kumthekar, M. W., *J. Catal.* **149,** 390 (1994).
17. Ramis, G., Busca, G., Bregani, F., and Forzatti, P., *in* "Catalytic Science and Technology," (S. Yoshida, N. Takezawa and T. Ono, Eds.), Vol. 1, p. 189. Kondasha, Tokyo, 1991.
18. Ramis, G., Busca, G., Bregani, F., and Forzatti, P., *Appl. Catal.* **64,** 259 (1990).
19. Lietti, L., Svachula, J., Forzatti, P., Busca, G., Ramis, G., and Bregani, F., *Catal. Today* **17,** 131 (1993).
20. Willey, R. J., Eldridge, J. W., and Kittrell, J. R., *Ind. Eng. Chem. Prod. Res. Dev.* **24,** 226 (1985).
21. Went, G. T., Li-Jen Leu, and Bell, A. T., *J. Catal.* **134,** 479 (1992); Went, G. T., Li-Jen Leu, Lombardo, S. J., and Bell, A. T., *J. Phys. Chem.* **96,** 2235 (1992).
22. Duffy, B. L., Curry-Hyde, H. E., Cant, N. W., and Nelson, P. F., *J. Catal.* **149,** 11 (1994).
23. Tufano, V., and Turco, M., *Appl. Catal. B: Envir.* **2,** 9 (1993).
24. Gallardo Amores, J. M., Sanchez Escribano, V., Busca, G., and Lorenzelli, V., *J. Mater. Chem.* **4,** 965 (1994).
25. Willey, R. J., Oliver, S. A., Oliveri, G., and Busca, G., *J. Mater. Res.* **8,** 1418 (1993).
26. Ciambelli, P., Bagnasco, G., Lisi, L., Turco, M., Chiarello, G., Musci,

M., Notaro, M., Robba, D., and Gretti, P., *Appl. Catal. B: Envir.* **1,** 61 (1992); Turco, M., work in progress.
27. Centi, G., Nigro, C., Perathoner, S., and Stella, G., *Catal. Today* **17,** 159 (1993).
28. Wollner, A., Lange, F., Schmelz, H., and Knozinger, H., *Appl. Catal. A: General* **94,** 181 (1993).
29. Kato, A., Matsuda, S., Nakajima, F., Imanari, M., and Watanabe, Y., *J. Phys. Chem.* **85,** 1710 (1981).
30. Janssen, F. J. J. G., and van den Kerkhof, F. M. G., *Kema Scientific and Technical Reports* **3,** 71 (1985).
31. Bauerle, G. L., Wu, S. C., and Nobe, K., *Ind. Eng. Chem. Prod. Res. Dev.* **14,** 268 (1975).
32. Willey, R. J., Lai, H., and Peri, J. B., *J. Catal.* **130,** 319 (1991).
33. Amiridis, M. D., Puglisi, F., Dumesic, J. A., Millman, W. S., and Nan-Yu Topsoe, *J. Catal.* **142,** 572 (1993).
34. Germain, J. E., and Perez, R., *Bull. Soc. Chim. Fr.* 2042 (1972).
35. Wu, Y., Yu, Y., Dou, B., Wang, C., Xie, X., Yu, Z., Fan, S., and Wang, L., *J. Catal.* **120,** 88 (1989).
36. Wong, W. C., and Nobe, K., *Ind. Eng. Chem. Prod. Res. Dev.* **23,** 564 (1984).
37. Went, G. T., Li-Jen Leu, Rosin, R. R., and Bell, A. T., *J. Catal.* **134,** 492 (1992).
38. Lietti, L., and Forzatti, P., *J. Catal.* **147,** 241 (1994).
39. Alemany, L. J., Lietti, L., Ferlazzo, N., Forzatti, P., Busca, G., Giamello, E., and Bregani, F., *J. Catal.* in press.
40. Tsyganenko, A. A., Pozdnyakov, D. V., and Filimonov, V. N., *J. Mol. Struct.* **29,** 299 (1975).
41. Busca, G., Saussey, H., Saur, O., Lavalley, J. C., and Lorenzelli, V., *Appl. Catal.* **14,** 245 (1985).
42. Ramis, G., Busca, G., Lorenzelli, V., and Forzatti, P., *Appl. Catal.* **64,** 243 (1990).
43. Busca, G., *J. Mol. Catal.* **43,** 225 (1987).
44. Sacconi, L., and Sabatini, A., *J. Inorg. Nucl. Chem.* **25,** 1389 (1963).
45. Sathyanarayana, D. N., and Nicholls, D., *Spectrochim. Acta Part A* **34,** 263 (1978).
46. Brill, R., Jiru, P., and Schulz, G., *Z. Phys. Chem. Neue Folge* **64,** 216 (1969).
47. Durig, J. R., Bush, S. F., and Mercer, E. E., *J. Chem. Phys.* **44,** 4238 (1966).
48. Gray, P., and Waddington, T. C., *Trans. Faraday Soc.* **53,** 901 (1957).
49. Martra, G., Borello, E., Giamello, E., and Coluccia, S., *in* "Acid-Base Catalysis II" (H. Hattori, M. Misono, and Y. Ono, Eds.), p. 169. Elsevier, Amsterdam, 1994.
50. Laane, J., and Ohlsen, J. R., *Prog. Inorg. Chem.* **28,** 465 (1980).
51. Spoto, G., Bordiga, S., Scarano, D., and Zecchina, A., *Catal. Lett.* **13,** 39 (1992).
52. Lorenzelli, V., and Busca, G., *Mater. Chem. Phys.* **13,** 261 (1985).
53. Kagami, S., Onishi, T., and Tamaru, K., *J. Chem. Soc. Faraday Trans. 1* **80,** 29 (1984).
54. Vergnon, P., and Batis, H., *Bull. Soc. Chim. Fr.* 266 (1984).
55. Busca, G., Ramis, G., and Lorenzelli, V., *J. Mol. Catal.* **50,** 231 (1989).
56. Lin-Vien, D., Colthup, N. B., Fateley, W. G., and Grasselli, J. G., "The Handbook of Infrared and Raman Characteristic Frequencies of Organic Molecules." Academic Press, New York, 1991.
57. Williamson, W. B., Flenige, D. R., and Lunsford, J. H., *J. Catal.* **37,** 258 (1975).
58. Biermann, J. J. P., and Janssen, F. J. J. G., *Appl. Catal. A: General* **86,** 165 (1992).
59. de Boer, M., Huisman, H., Mos, R. J. M., Leliveld, R. G., van Dillen, A. J., and Geus, J. W., *Catal. Today* **17,** 189 (1993).
60. Stedman, G., *Adv. Inorg. Chem. Radiochem.* **22,** 113 (1979).
61. Mars, P., and van Krevelen, W., *Eng. Sci.* **3,** 41 (1954).
62. Escalona-Platero, E., Coluccia, S., and Zecchina, A., *J. Catal.* **103,** 270 (1987).
63. Lintz, H. G., and Turek, T., *Appl. Catal. A: General* **85,** 13 (1992).
64. Busca, G., and Ramis, G., *in* "Proceedings, Italian Conference on Chemical and Process Engineering, Firenze, 1993," p. 91. AIDIC, Milano, 1994.